RSC Applied Polymers

ROYAL SOCIETY OF CHEMISTRY

PAPER

View Article Online
View Journal | View Issue

Cite this: *RSC Appl. Polym.*, 2025, **3**, 885

Synthesis of an anion exchange resin for enhanced PFAS adsorption in water treatment†

Leila Khazdooz,‡ Amin Zarei‡ and Alireza Abbaspourrad *

Per- and polyfluoroalkyl substances (PFASs) are a class of toxic, bioaccumulative, and persistent chemicals that pollute natural water sources and the environment, new materials and methods to remove them from water are needed. Anion exchange resins adsorb PFASs through strong electrostatic interactions with negatively charged PFAS molecules with high selectivity and removal efficiency from contaminated water. A series of cross-linked anion exchange resins in the form of polymeric beads were synthesized *via* inverse suspension polymerization using commercially available cationic monomers, (3-acrylamidopropyl)-trimethylammonium chloride (APTMAC) or diallyldimethylammonium chloride (DADMAC), and the crosslinker, *N*,*N*′-methylenebisacrylamide (BisAAm).The resins were evaluated for their ability to remove perfluorooctanoic acid (PFOA) from water and the DADMAC based resin (DR4) with 10 w/w% crosslinker showed the highest efficiency. DR4 exhibits high adsorption capacities of 3300 mg g^{-1} for PFOA, coupled with rapid adsorption kinetics, achieving equilibrium within an hour. Minimum interference effects from salts, pH variations, and natural organic matter (NOM) were observed and the competitive adsorption study indicated that the presence of other PFASs had no impact on the adsorption efficiency of DR4. DR4 was washed and reused, maintaining its performance after five consecutive PFOA adsorption and desorption cycles.

Received 7th February 2025,
Accepted 1st May 2025

DOI: 10.1039/d5lp00035a

rsc.li/rscapplpolym

1. Introduction

Per- and polyfluoroalkyl substances (PFASs) have become ubiquitous in natural waters and because they are chemically and thermally stable as well as resistant to degradation, they are also found in drinking water.[1] Recent research indicates that these compounds progressively bioaccumulate in human tissues such as the brain, liver, lungs, bones, and kidneys, leading to functional impairments.[2–5] Furthermore, PFAS exposure can disrupt normal endocrine functions, weaken the immune system, impair fertility, elevate cholesterol levels, and decrease birth weight.[6–10] The International Agency for Research on Cancer (IARC) and the Environmental Protection Agency have classified PFASs as potentially carcinogenic,[11] highlighting their significant threat to both the environment and human health. Unfortunately, concentrations of two major PFASs, perfluorooctanoic acid (PFOA) and perfluorooctane sulfonic acid (PFOS), have risen in natural water sources, with contaminated groundwater recording high levels exceeding 1000 ng L^{-1} for PFOA and PFOS,[12] contrary to the EU Environmental Protection Agency's recommended advisory level of less than 70 ng L^{-1}.[13,14]

Adsorption emerges as one of the most efficient, environmentally sustainable, and economically viable techniques for removing PFASs from water.[1,15–18] Multiple types of solid state adsorbents have been reported as effective for the removal of PFASs from aqueous solutions including anion-exchange resins,[19–23] porous organic networks,[14,24–26] and covalent organic frameworks (COFs).[11,12,27–30] These materials typically offer large specific surface areas, suitable pore sizes, and specific functional groups that enhance adsorption efficiency. Some of these adsorbents, however, exhibit limitations such as low capacity, slow adsorption rates, and structural changes at different pH levels. Additionally, most of these porous materials are synthesized as a benchtop scale through several complicated steps.

Anionic exchange resins like IRA67, IRA400, and IRA910 are effective adsorbents for removing PFASs from water and are widely used in industry due to their cost-effectiveness, superior adsorption capacity, and high regeneration capability.[20,22,31]

Department of Food Science, College of Agriculture & Life Sciences, Cornell University, Stocking Hall, Ithaca, New York, 14853, USA. E-mail: Alireza@cornell.edu

†Electronic supplementary information (ESI) available: Detailed table of synthetic preparations for each resin. Additional figures including FTIR, TGA, SEM of resins and Langmuir and Freundlich isotherms for adsorption of PFAS onto DR4. Comparison table of previously published adsorbents for PFAS with DR4 resin. Raw data used to create the visual elements can be found at: https://zenodo.org/records/13984331. See DOI: https://doi.org/10.1039/d5lp00035a

‡These authors contributed equally to this work.

However, they still suffer from slow adsorption kinetics and extended equilibrium times. A polymer with specialized multi-functional groups, including positive charges, hydrophobic carbon chains, hydrogen bonding sites, and fluorophilic interactions could address this problem.[14,28,29,32–37] Another crucial factor in enhancing PFAS adsorption efficiency is improving water wettability through increased hydrophilicity. This enhancement facilitates the mass transfer of PFASs toward the adsorbent's capture sites.[14] Considering these factors, we synthesized two cross-linked anion exchange resins starting with diallyldimethylammonium chloride (DADMAC) and (3-acrylamidopropyl)-trimethylammonium chloride (APTMAC), two commercially available cationic monomers, and cross-linked the resins using *N*,*N*′-methylenebisacrylamide (BisAAm) (Scheme 1). Polyvinyl alcohol (PVOH) was used as a porogen to enhance the porosity of the resins. Structurally, the quaternary ammonium groups impart a positive charge to the resins, while the NH groups provide hydrogen bonding sites. Compared to the APTMAC resin (AR), the DADMAC resin (DR) showed better affinity for removing PFOA from contaminated water. This is due to the incorporation of hydrogen bonding sites that, combined with the positive charge of quaternary ammonium moieties present in DADMAC, improved swelling in water which synergistically aids in the removal of PFASs. DR4 also showed high adsorption capacity (3300 mg g^{-1}) for PFOA removal from aqueous solutions.

2. Materials and methods

2.1. Materials

Diallyldimethylammonium chloride (DADMAC) aqueous solution (65 w/w%), ammonium persulfate (APS) (≥98%), polyvinyl alcohol (PVOH) (fully hydrolyzed, MW ≈ 60 000 g mol^{-1}), were purchased and used as received from Sigma Aldrich (St Louis, MO, USA). (3-Acrylamidopropyl)-trimethylammonium chloride (APTMAC) aqueous solution (75 w/w%) was purchased from Santa Cruz biotechnology (Dallas, TX, USA). *N*,*N*-Methylenebisacrylamide (BisAAm) (>99%) was purchased from Alfa Aesar (Haverhill, MA, USA). Dioctyl sulfosuccinate (AOT) (96%) was purchased from VWR (Radnor, PA, USA). Perfluorodecanoic acid (98%), perfluorooctanoic acid (95%), and perfluorooctane sulfonic acid (40% solution in water) were purchased from Sigma-Aldrich (St Louis, MO, USA). Perfluorohexanoic acid (98%) was purchased from AmBeed (Arlington Heights, IL, USA) and perfluorobutanoic acid (a

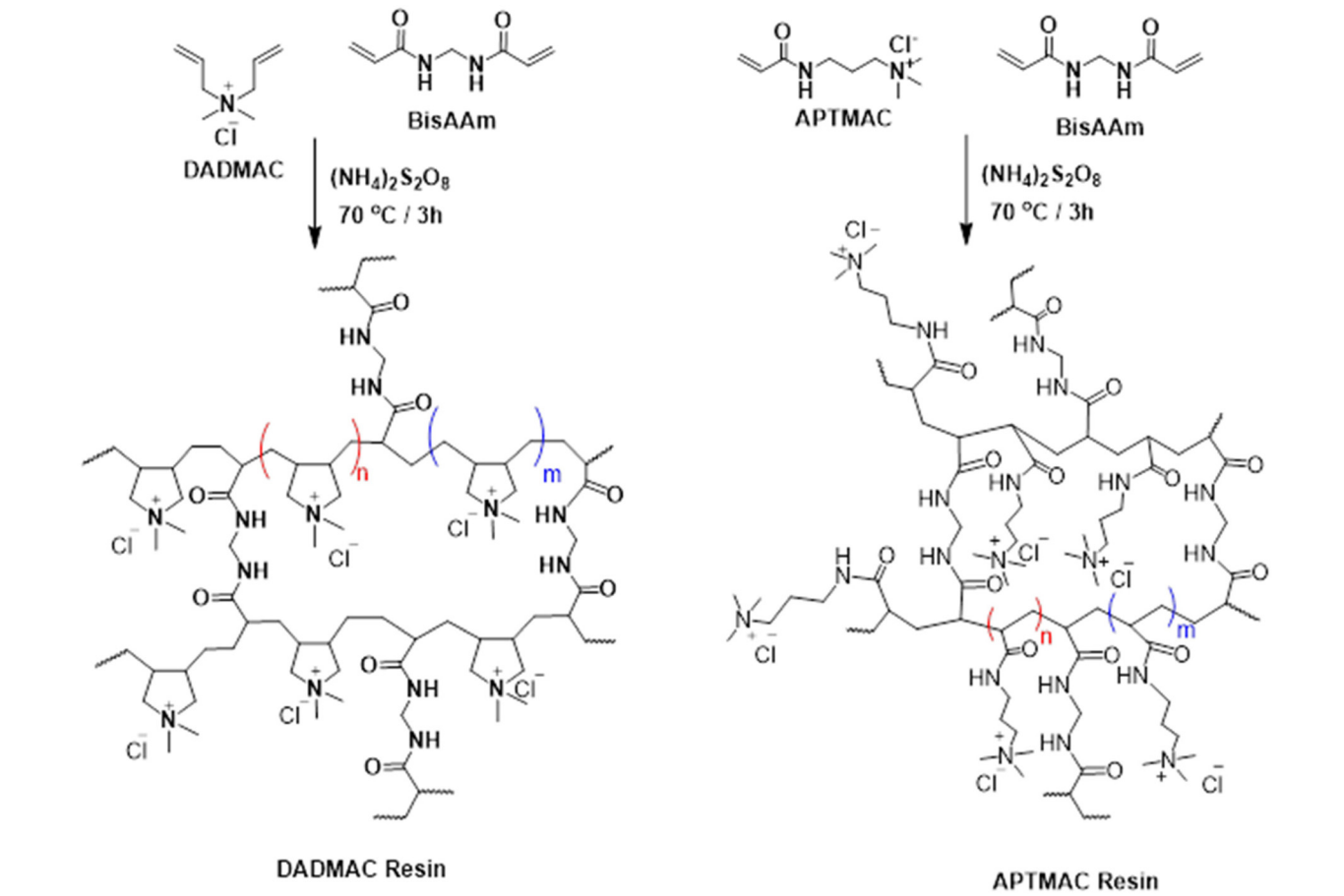

Scheme 1 The reaction of *N*,*N*-idmethylenebisacrylamide (BisAAm) with either diallyldimethylammonium chloride (DADMAC) or (3-acrylamidopropyl)-trimethylammonium chloride (APTMAC) to synthesize DADMAC resins or APTMAC resins.

0.5 mol L^{-1} solution in water with LC-MS grade) was purchased from TCI (Montgomeryville, PA, USA). All solvents such as ethanol, methanol, analytical grade methanol, were purchased from Sigma-Aldrich (St Louis, MO, USA) and used as received. Mazola corn oil was purchased from a local market (Ithaca, NY, USA).

2.2. Characterization

Attenuated total reflectance Fourier transform infrared spectra (ATR–FTIR) were measured with a Shimadzu IRAffinity-1S spectrophotometer at the range from 400 to 4000 cm^{-1}. Thermogravimetric Analysis (TGA) was performed using a Q500 Thermogravimetric Analyzer (TA Instruments, New Castle, DE, USA) under nitrogen atmosphere and a heating rate of 10 °C min^{-1} in the range of 25–800 °C. Scanning electron microscopy (SEM) was performed using a Zeiss Gemini 500 field emission SEM, samples were coated with a thin carbon layer using a Leica EM SCD 500 sputter system under an argon atmosphere at a pressure of 10^{-4} mbar. X-ray Photoelectron Spectroscopy (XPS) was conducted using a Scienta Omicron ESCA 2SR instrument under an operating pressure of approximately 1×10^{-9} Torr. Wide/survey scans were performed with a pass energy of 200 eV.

2.3. Liquid chromatography/mass spectrometry (LC-MS) conditions

Liquid chromatography (LC, Agilent 1100 series) coupled with a mass spectrometer (MS) was used to analyze PFOA samples. A Phenomenex Luna Omega LC column (100 × 4.6 mm, 3 μm, polar Luna C18, 100 Å pore size) was used at a flow rate of 0.4 mL min^{-1}. The samples were filtered through a 13 mm syringe filter polyvinylidene fluoride (PVDF) with a 0.22 μm pore size then were injected. Mobile phases A (Milli-Q water containing 20 mM ammonium acetate), and mobile phases B (methanol) were used for LC column elution. A gradient elution over a 14-minute run time was applied as follows: 0 to 1 min, 60% A; 1 to 5 min, 60% to 5% A; 5 to 10 min, 5% A; 10 to 12 min, 5% to 60% B; 12 to 14 min, 60% A. The injection volume was 10 μL.

The mass spectrometer (Finnigan LTQ) was equipped with an electrospray interface (ESI) operating in positive ion mode. Sheath gas flow rate of 50 arbitrary units, capillary temperature at 350 °C, capillary voltage at 41.0 V, spray voltage at 4.00 kV, and tube lens at 125.0 V are the optimized parameters that are set for mass spectrometer. Quantitative analysis of samples with initial concentrations below 20 μg L^{-1} was performed by Pace Analytical Services Co. All details of the sample preparation methods and equipment used by Pace are based on our previous work.[38] All measurements were conducted in triplicate.

2.4. Inverse suspension polymerization for resins synthesis

All resins were synthesized using inverse suspension polymerization according to our previous work.[39,40] The formulation of each resin can be found in Table 1 and the specific quantities of the monomer, crosslinker, porogen, AOT, and APS for synthesis of each resin were summarized in Table S1.† All synthesized resins were characterized by FTIR, and TGA analysis (Fig. S1–S12†).

Table 1 The formulation for the synthesized ion exchange resins for PFAS adsorption[a]

Resin name	AR1	AR2	AR3	DR4	DR5	DR6	DR7
APTMAC (mol%)	100	100	100	—	—	—	—
DADMAC (mol%)	—	—	—	100	100	100	100
Bis-AAM (mol%)[b]	10	30	40	10	30	40	10
Porogen (w/w%)[c]	5	5	5	5	5	5	—

[a] For all the resins synthesis, APS (2 mol% of monomer) as initiator, AOT (1 mol% of monomer) as a surfactant, MeOH (4 times mass of Bis-AAM), and oil/water ratio (70 : 30 v : v) were used. [b] Bis-AAM (mol % of APTMAC or DADMAC) was added as a crosslinker. [c] PVOH (5 w/w% of monomer and Bis-AAM) was added as a porogen.

A typical synthesis for resin DR4. A 200 mL glass bottle was charged by 37.3 g (65 w/w% aqueous solution, 150 mmol) of DADMAC, 13.3 mL of PVOH (10.0 w/v% in water,), 2.30 g (15 mmol) of BisAAm, 0.668 g (1.5 mmol) AOT, and 10.0 mL methanol. The mixture was sonicated for 15–30 min at 40 °C to obtain a clear aqueous solution. After cooling to room temperature 0.684 g (3 mmol) of APS as initiator was added to the solution and mixed gently to prevent foam formation. A 500 mL glass reactor with mechanical stirrer was charged with 150.0 mL of corn oil. The aqueous phase was rapidly added to the stirred corn oil at room temperature (25 °C). The temperature then increased from 25 °C to 70 °C over 15 min and held at 70 °C for 3 h. After cooling, the resin beads were washed with hexane, ethanol, and deionized (DI) water as described in our previous work,[39] to remove unreacted monomers, porogens, initiators, and surfactants, then freeze-dried for use in adsorption experiments.

2.5. PFAS adsorption studies

2.5.1. Adsorption studies of PFOA using synthesized resins. Adsorption experiments by the synthesized resins were conducted in 500 mL plastic bottles. To these studies, 10 mg of each resin was added to 100 mL of PFOA solution (5 mg L^{-1}). After that, the samples were shaken on a rocking shaker at 80 rpm under ambient temperature for 1 h. Then, 1 mL of each sample was filtered out with a 0.22 μm syringe filter (PVDF), and the filtrate was analyzed by LC/MS. Control experiments were carried out under the same conditions without using any resin.

The PFOA removal efficiency for each resin was calculated according to eqn (1), and the amount of PFOA adsorbed on the adsorbent was calculated by eqn (2),

$$\text{Removal}\,\% = \frac{(C_0 - C_t) \times 100\%}{C_0} \quad (1)$$

$$q_t = \frac{C_0 - C_t}{C_A} \quad (2)$$

where C_0 (μg L^{-1}) and C_t (μg L^{-1}) are the initial concentration of PFOA and PFOA concentration at a given time respectively,

q_t (mg g^{-1}) is the amount of adsorbed PFOA on the resin at specified times, and C_A (mg L^{-1}) is the adsorbent concentration.

2.5.2. Time-dependent and kinetic studies of PFOA adsorption using resin DR4. To kinetic studies four different groups of experiments were carried out. The amount of resin DR4, volume of solution, and PFOA solution concentration for each group can be found in Fig. 5.

A typical kinetic study for group I. A 500 mL plastic bottle was charged with 10 mg of resin DR4, and 100 mL of PFOA solution with 10 mg L^{-1} concentration. The mixture was shaken at room temperature by a rocking shaker at 80 rpm. At specified time points (5, 10, 15, 20, 30, 45, 60, 90, 120, and 180 min) 1 mL of each sample was collected, filtered, and analyzed by LC/MS. The kinetics of the PFOA adsorption by each group was fitted by Ho and McKay's pseudo-second-order adsorption model in a linearized form.[38]

2.5.3. PFOA adsorption Langmuir isotherm study. The PFOA adsorption isotherm experiments were carried out in 500 mL plastic bottles containing 100 mL of different concentrations of PFOA standard solutions. Various initial concentrations of PFOA in each bottle included 10, 20, 50, 70, 100, 200, 600, and 800 mg L^{-1}. For each sample, 10 mg of resin DR4 was added. The experiments were carried out at room temperature and shaken on a rocking shaker for 24 h. Subsequently, 1.0 mL of each sample was collected, filtered, and analyzed to measure the remaining PFOA content. The adsorption isotherms were studied by Langmuir and Freundlich models.[38]

2.5.4. Reusability of resin DR4. The reusability experiments were performed in a 500 mL plastic bottle by adding 20 mg of resin DR4 to 200 mL PFOA solution at a concentration of 1 mg L^{-1}. The sample was shaken at room temperature by a rocking shaker at 80 rpm for 1 h. Subsequently, the solution was filtered through the sintered glass filter (20 μ size). The used resin was then rinsed with 100 mL of solution (70% methanol : 30% NaCl (1%)) and consequently washed with MQ-water (2 × 10 mL). The resin does not need any activation or any special regeneration before reusing.

3. Results and discussion

3.1 Resin synthesis and characterization

We synthesized various anion exchange resins by inverse suspension polymerization of APTMAC and DADMAC. For all anion exchange resins BisAAm was used as a crosslinker. For the synthesis of these resins sodium di-2-ethylhexylsulfosuccinate (AOT) as an anionic surfactant was used to place most of the cationic monomers (APTMAC and DADMAC) on the surface of resins and increase the functionality of ammonium groups on the surface of the corresponding resins.[40] The absence of a surfactant in inverse suspension polymerization can result in severe delamination due to phase separation within the aqueous droplets. To mitigate this issue, a surfactant is used to facilitate the participation of hydrophilic monomers at the interface, thereby ensuring their integration into the resin surface.[40]

We synthesized three anion exchange resins (AR1, AR2, AR3) by using APTMAC and four anion exchange resins (DR4, DR5, DR6, DR7) by using DADMAC, the formulations of synthesized resins are summarized in Table 1, with additional details in Table S1.† To study the effect of crosslinker we increased the amount of Bis-AAM from 10 to 40% in APTMAC resins (AR1–AR3) and in DADMAC resins (DR4–DR6). In all mentioned synthesized resins PVOH (5 w/w% of both monomer and crosslinker) was used as a porogen to increase the porosity. To observe the effect of porosity in the resins, resin DR7 was synthesized using the same formulation as resin DR4 but without using porogen.

All synthesized resins were characterized by FT-IR and TGA. The FT-IR spectrum of resins confirmed the functional groups and showed the stretching vibrations of free N–H bonds in 3375–3248 cm^{-1} regions.[41] A strong band at around 1643 cm^{-1} corresponds to the stretching C═O bond of the amide groups (Fig. S1–S6†). To assess the thermal stability of the synthesized resins, Thermogravimetric Analysis (TGA) was performed under a nitrogen atmosphere with a heating rate of 10 °C min^{-1}, over a temperature range of 25 °C to 800 °C. All samples were dried overnight under vacuum at 60 °C; nevertheless, approximately 20% of its total mass was attributed to adsorbed atmospheric humidity. This relatively high moisture adsorption can be ascribed to the hydrophilic nature of the resin.[40] The TGA thermograms showed a similar pattern for APTMAC resins (AR1–AR3) and also we observed a similar pattern for DADMAC resins (DR4–AR7). In all resins the first weight loss occurred around 300 °C which is related to the degradation of the crosslinking segments (Bis-AAM) within the polymer structure (Fig. S7–S12†).

We studied the performance of all synthesized resins for PFOA adsorption, and DR4 demonstrated the best PFOA adsorption. Therefore, we fully characterized the functional groups, thermal stability, and surface composition of DR4.

The FT-IR spectrum of the DR4 exhibited stretching vibrations of N–H bonds at 3375 and 3248 cm^{-1} (Fig. 1a), associated with the secondary amide groups of the crosslinker in the resin.[41] The stretching vibrations of the aliphatic C–H bonds were observed around 2935 cm^{-1}. A strong band at 1647 cm^{-1} corresponds to the stretching C═O bond of the amide groups. A band at 1527 cm^{-1} is attributed to the N–H bending vibration of the amide groups. The bending vibration of CH_2 groups, indicative of the polymerization of DADMAC, was observed at 1473 cm^{-1}. Lastly, a broad band in the 800–600 cm^{-1} region confirms the out-of-plane N–H wagging vibrations.[41] The TGA thermograms and the rate of degradation as a function of temperature are illustrated in Fig. 1b. Typical of synthesized resins, approximately 20% of its total mass was attributed to adsorbed atmospheric humidity. The initial major weight loss, observed around 320 °C, corresponds to the degradation of the crosslinking segments (Bis-AAM) within the DR4 structure. The subsequent significant change in the degradation rate, noted at approximately 475 °C, signifies the degradation of the DADMAC subunit.[42]

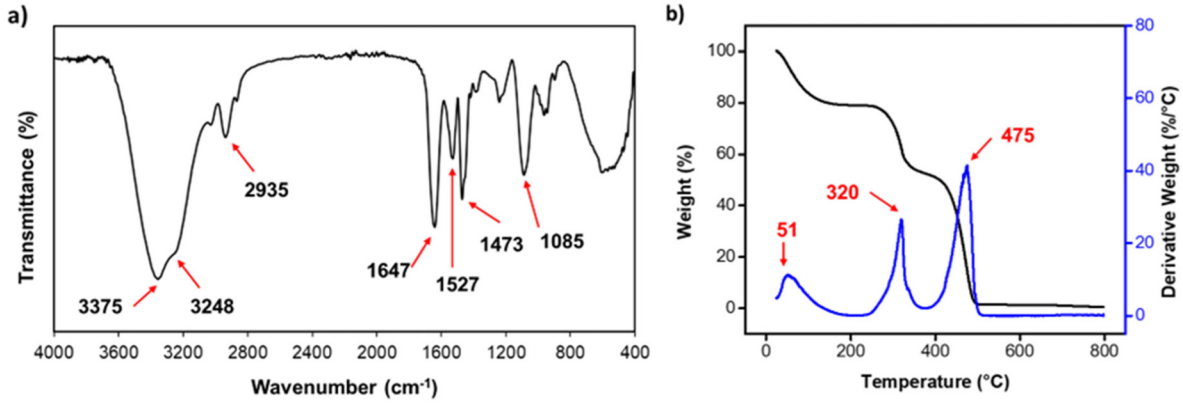

Fig. 1 (a) FTIR spectrum of resin DR4. (b) TGA/DTG thermograms of resin DR4.

Finally, X-ray photoelectron spectroscopy (XPS) was used to investigate the chemical states of surface elements, confirming the presence of C, N, O, and Cl in the DR4 structure (Fig. 2a). The deconvolution of the C 1s spectrum revealed a distinct peak at a binding energy of 284.6 eV, indicating C–C bonds in the DR4 structure (Fig. 2b). The corresponding binding energies for C–N and C═O bonds were observed at 285.8 eV and 286.5 eV, respectively. The N 1s spectrum showed two peaks at 399.1 eV and 401.9 eV, attributed to N–C in the crosslinker section and $^{+}$N–C in quaternary ammonium moieties, respectively (Fig. 2c).[43] A peak at 531.5 eV, implying the presence of oxygen, was assigned to the C═O groups (Fig. 2d). Additionally, peaks observed at 196.6 eV, 198.2 eV, and 268.1 eV were identified as Cl $2p_{3/2}$, Cl $2p_{1/2}$, and Cl 2s, respectively, confirming the presence of chloride anions in the resin DR4 (Fig. 2e and f).[43]

To assess the impact of adding a porogen during synthesis, the morphology of DR4 and DR7 resins was studied using scanning electron microscopy (SEM). The SEM images revealed that both resins exhibited spherical shapes beads in the range of 20 to 100 μm. However, DR4 displayed significant surface roughness and porosity attributable to the porogen (PVOH) used during its synthesis (Fig. 3a–c). In contrast, the surface of DR7, synthesized without the porogen, was completely smooth and lacked any roughness (Fig. 3d–f). This structural distinction accounts for the adsorption performance of DR4 for PFOA which is noticeably higher than DR7.

3.2 PFOA removal from aqueous solutions

After synthesizing the anion exchange resins, they were used to remove PFOA from aqueous solutions. In these experiments, 10 mg of each resin was separately added to 100 mL of an aqueous PFOA solution (5 mg L^{-1}). After 1 hour of exposure at room temperature, the PFOA remaining in the solution was measured using LC-MS. The maximum removal efficiency was achieved using DR4, which removed 99.6% of the PFOA (Fig. 4a). Although both APTEMAC and DADMAC resins have positive sites in their structures to increase the affinity between the resins and PFOA, the DADMAC resins demonstrated higher removal efficiency than the APTEMAC resins.

To explain the difference in adsorption, the swelling of APTEMAC and DADMAC resins was investigated, water swelling is enhanced by higher hydrophilicity of adsorbent particles and the presence of highly accessible functionalized capturing sites. Higher swelling accelerates the mass transfer of PFASs towards the adsorbents in aqueous solutions, thereby increasing adsorption of PFASs from water.[14] The swelling of APTEMAC and DADMAC resins was investigated by comparing the behavior of each resin (100 mg) in water (Fig. 4b). The swelling percentage was determined using the equation: swelling = $[(W_2 - W_1)/W_1] \times 100$, where W_1 represents the weight of the dry resin and W_2 represents the weight of the swollen resin.[39,44] DADMAC resins exhibited higher swelling than APTEMAC resins. This enhanced swelling likely accounts for the increased PFOA uptake observed with DADMAC resins. To test this, the proportion of the crosslinker was increased, which reduced the number of positive capturing sites and led to decreased swelling and, consequently, lower PFOA adsorption. The optimal amount of Bis-AAM was determined to be 10 mol%. Additionally, the use of PVOH as a porogen in the synthesis of DR4, compared to DR7, further improved both the swelling and adsorption efficiency of the resin.

3.3 PFOA adsorption using DR4

DR4 was determined to have the best adsorption of PFOA from water and therefore was used for all further studies. Energy-dispersive X-ray spectroscopy (EDS) and FT-IR were used to verify the presence of adsorbed PFOA on DR4. EDS mapping demonstrated a uniform distribution of fluorine across the surface of DR4 (Fig. S13†). Additionally, FT-IR analysis of the adsorbed PFOA on DR4 displayed a distinct band at 1690 cm^{-1}, corresponding to the stretching vibration of the carbonyl functional group of PFOA (Fig. S14†). Furthermore, bands observed at approximately 1199 and 1143 cm^{-1} were attributed to the stretching vibrations of the CF_3 and CF_2 groups of PFOA, respectively.[41]

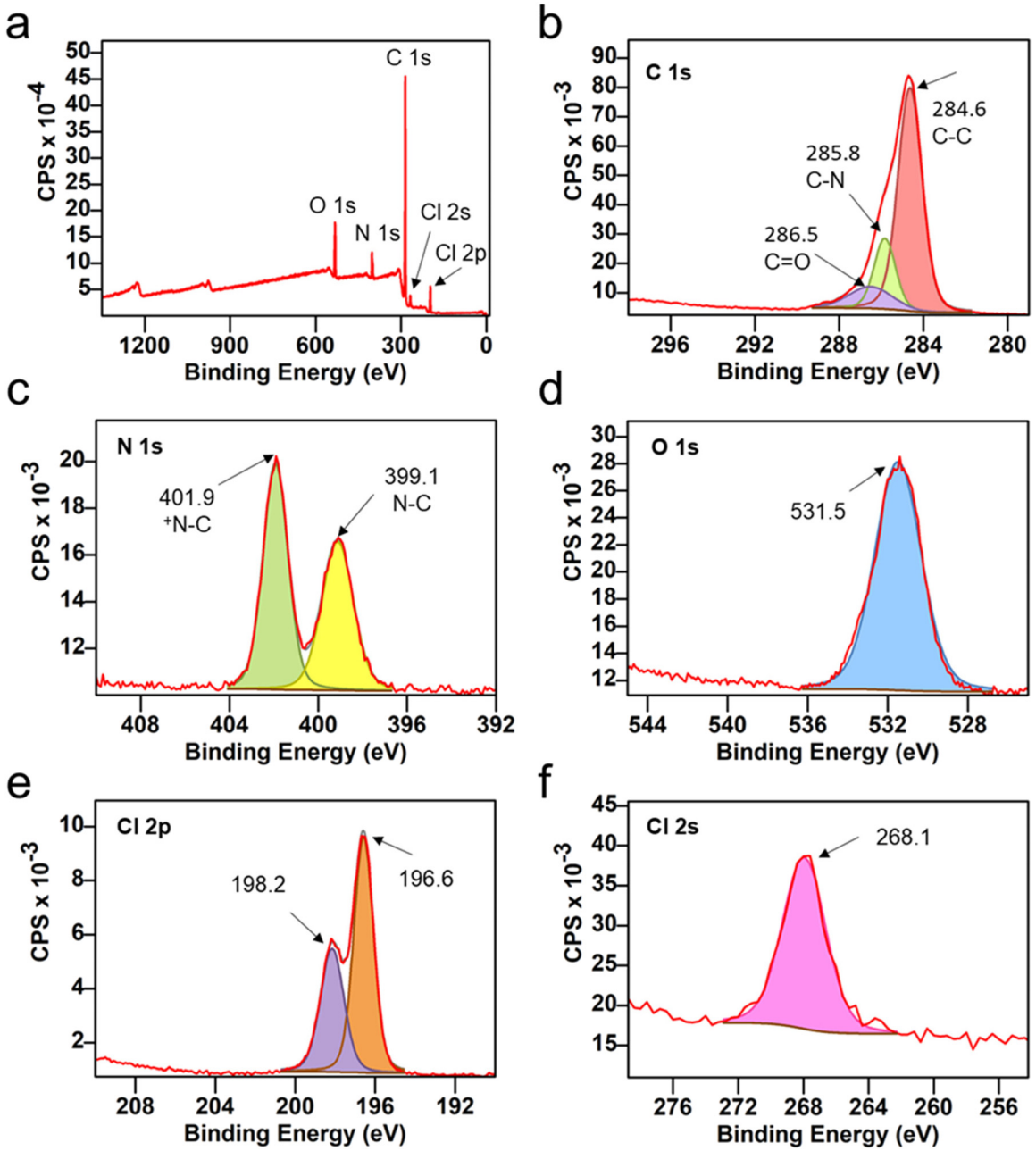

Fig. 2 (a) High-resolution XPS analysis of resin DR4. Deconvoluted profiles of (b) C 1s, (Residual STD: 1.7) (c) N 1s, (Residual STD: 0.95) (d) O 1s (e) Cl 2p, (Residual STD: 1.2), and (f) Cl 2s.

To assess the resin DR4's performance, toward PFOA adsorption, the time-dependent and kinetic behavior were assessed for PFOA adsorption at various concentrations over a 2 h period (Fig. 5a). The selection of 0.2 to 10 mg L^{-1} for PFOA solutions was designed to examine adsorption kinetics across a broad concentration range. Regardless of the PFOA concentration, the time-dependent studies demonstrated exceptional PFOA removal, exceeding 98% within 30 minutes using DR4 (Fig. 5b). DR4, with a particle size range of 20–100 μm (Fig. 3a), exhibited rapid adsorption kinetics, achieving greater than 99% PFOA adsorption in less than 60 minutes. This rapid performance may be attributed to its smaller particle size, and thus larger surface area, when compared to commercial anionic exchange resins such as IRA67, IRA400, and IRA910, which typically have particle sizes ranging from 0.3 to 1.2 mm.[20,22,31] The kinetics of DR4 at each PFOA concentration were modeled using the linear pseudo-second-order kinetic model (Fig. 5c), and the corresponding rate constants were determined (Fig. 5a). These findings underscore the rapid and efficient adsorption capabilities of DR4, establishing it as an effective anionic exchange resin for the removal of PFOA from water in different concentrations (Fig. 5a, entries I–III). Further, increasing the adsorbent amount improved the adsorption rate (Fig. 5a, entries III–IV).

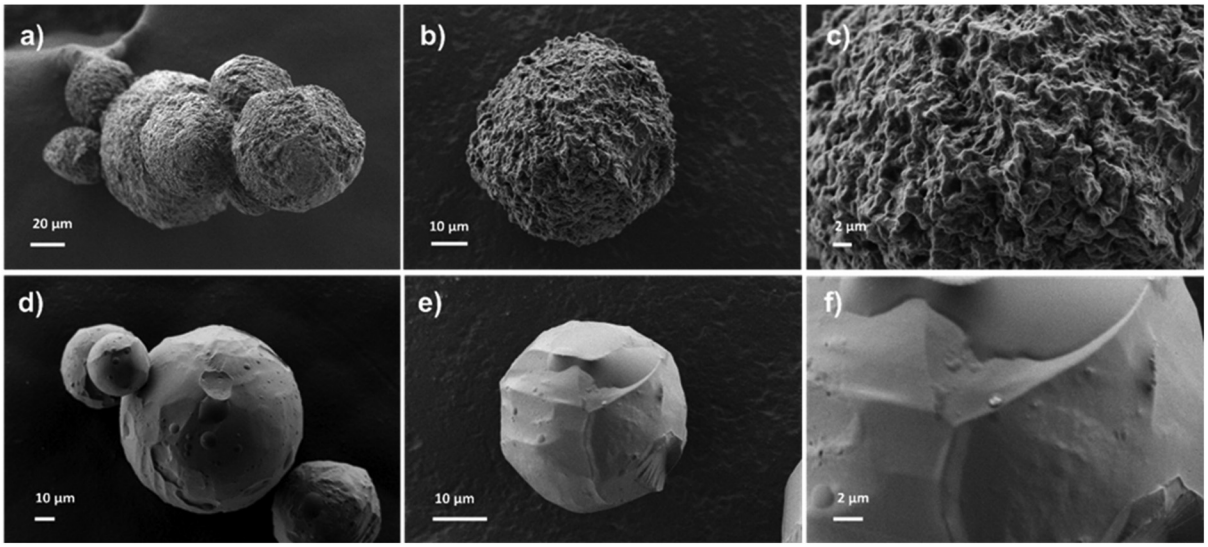

Fig. 3 (a–c) SEM images of resin DR4 revealing spherical particle shapes and roughness. (d–f) SEM images of resin DR7 revealing spherical particle shapes and smooth surface.

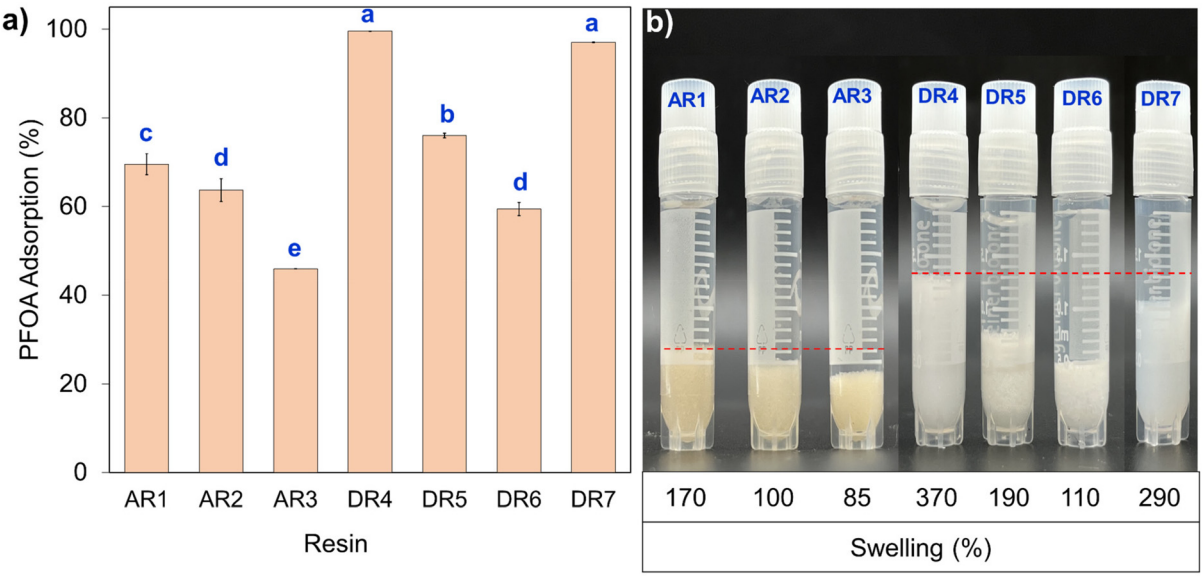

Fig. 4 (a) The efficiency of APTEMAC and DADMAC resins for the adsorption of PFOA from water. Different letters indicate significantly different values between groups as analyzed by one-way ANOVA with Tukey *post-hoc* test ($p < 0.050$). (b) The visual observation of the swelling of APTEMAC and DADMAC resins in water. Red dashed lines indicate top of the highest swelled resin levels for comparison.

The capacity of DR4 for PFOA removal from water was investigated. An adsorption isotherm was constructed using 10 mg of resin and PFOA solutions ranging from 1 to 800 mg L^{-1} (Fig. S15†). The adsorption isotherm exhibited an excellent fit with the Langmuir model, demonstrating remarkable alignment with a correlation coefficient of approximately 0.97 (Fig. S16†). Based on the Langmuir model, the estimated maximum adsorption capacity (Q_m) for DR4 was determined to be 3300 mg g^{-1}, representing the highest capacity for PFOA adsorption among reported anionic exchange resins and porous materials (Table S2†). Additionally, the affinity coefficient (K_L) was calculated to be 62 100 L mol^{-1}, indicating a strong affinity between DR4 and PFOA. The Freundlich isotherm, with a lower correlation coefficient of 0.82, did not fit the experimental data as well. The Freundlich constant (K_F) for DR4 was determined to be 756.7 (mg g^{-1}) (L $mg^{-1})^{(1/n)}$, where n was 3.6 (Fig. S17†).

The presence of quaternary ammonium groups with positive charges within the DR4 structure provide electrostatic and ion exchange interactions with PFOA that are likely the

a) Different experiments for kinetic studies of PFOA adsorption using resin DR4. *

Entry	FPOA concentration (mg/L) **	DR4 amount (mg)	Trendline equation	R^2	k (g/mg.h)
I	10	10	y=0.0098x+0.0004	0.9991	0.2401
II	1.0	10	y=0.1001x+0.0009	0.9999	11.13
III	0.2	10	y=0.5058x+0.0024	1	106.6
IV	0.2	30	y=1.506x +0.0024	1	945.0

* The kinetics were fitted with Ho and McKay's linear pseudo-second-order kinetic model.
** Volume of PFOA solution was 100 mL.

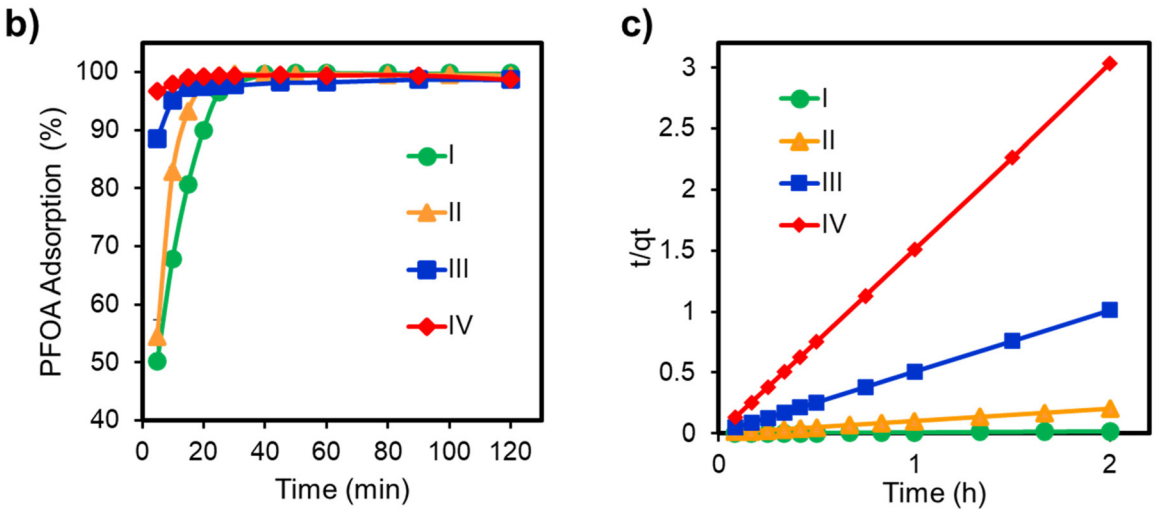

Fig. 5 (a) Different experiments for kinetic studies of PFOA adsorption. (b)Time-dependent PFOA adsorption of resin DR4 at different conditions (I: 100 mL PFOA (10 mg L^{-1})/10 mg DR4; II: 100 mL PFOA (1 mg L^{-1})/10 mg DR4; III: 100 mL PFOA (0.2 mg L^{-1})/10 mg DR4; IV: 100 mL PFOA (0.2 mg L^{-1})/30 mg DR4). (c) Linear fitting of kinetic adsorption of resin DR4 at different conditions.

primary mechanisms for adsorption.[20,22,31] Additionally, factors such as porosity, shape, and particle size of the adsorbents can significantly influence the efficiency of PFOA adsorption.[1,11,45] The high capacity and rapid kinetics of DR4 for PFOA removal can be attributed to its synthesis *via* inverse suspension polymerization. This polymerization method, involving cationic monomers in the presence of a suitable anionic surfactant and porogen, not only increases the number of active monomers on the surface but also enhances the polymer's porosity.[40] Consequently, the increased active capturing sites and improved porosity on the DR4 surface enhance the accessibility of active sites for PFOA adsorption, leading to a remarkable improvement in its efficiency compared to other reported anionic exchange resins.[20,22,31]

3.4 Effect of pH on PFOA adsorption

Since the pH of wastewater can vary widely from acidic to alkaline depending on the source of contamination, the absorption of PFOA was studied at different pH ranges. To illustrate the effect of pH on the adsorption efficiency of DR4, the removal of PFOA was investigated over a broad pH range from 3 to 9 (Fig. 6a). The pH was adjusted using 0.1 M solutions of HCl and NaOH. For each sample, the initial concentration of PFOA was maintained at 0.2 mg L^{-1}, with 10 mg of DR4 and an exposure time of 1 hour. The selected concentration of 0.2 mg L^{-1} is comparable to the reported maximum PFOA levels in industrial discharge, landfill leachate, wastewater, and contaminated groundwater, ensuring environmental relevance.[46,47]

Changing the pH between 5 and 8 had a minimal impact on the ability of DR4 to remove PFOA added to Milli-Q water. The highest removal efficiency was observed at pH 6, attributed to strong electrostatic interactions between PFOA and DR4. The pK_a of PFOA is 2.5,[48] indicating that at pH 6 it exists predominantly in its anionic form. This negative charge means that PFOA can effectively interact with the positively charged

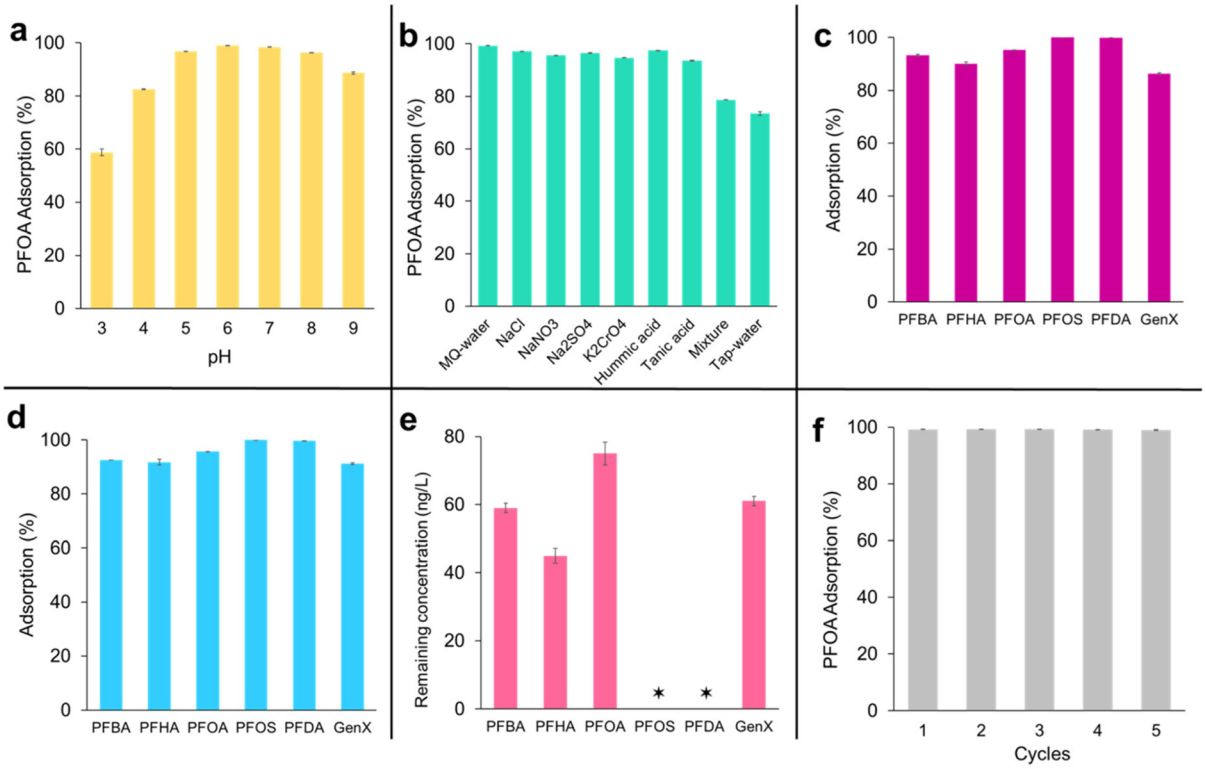

Fig. 6 (a) Effect of pH on the adsorption of PFOA by resin DR4 after 1 hour ($[PFOA]_0$ = 200 μg L^{-1}; DR4 = 10 mg, volume = 100 mL). (b) Effect of inorganic ions and natural organic matter (NOM) on the selective adsorption of PFOA by resin DR4 after 1 hour ($[PFOA]_0$ = 200 μg L^{-1}; DR4 = 10 mg, volume = 20 mL). (c) Adsorption of different PFASs by resin DR4 in a single solution after 1 hour ($[PFOA]_0$ = 20 μg L^{-1}; DR4 = 10 mg, volume = 100 mL). (d) Competitive adsorption of six different PFASs in Milli-Q water by resin DR4 in multi-solute solution after 1 hour (initial concentration of each PFAS = 20 μg L^{-1}; DR4 = 10 mg, volume = 100 mL). (e) Competitive adsorption of six different PFASs in drinking water by resin DR4 in multi-solute solution after 1 hour (initial concentration of each PFAS = 200 ng L^{-1}; DR4 = 50 mg, volume = 20 mL). (f) Reusability of resin DR4 in PFOA removal by consecutive adsorption experiments. All measurements were conducted in triplicate. Note: * indicates that the concentrations are not detected, and the standard error bars are not presented in those cases.

ammonium functional groups of DR4.[20] At pH 9, a decrease of approximately 10% in adsorption efficiency was observed, this is attributed to competition between hydroxide ions and PFOA with the DR4. This competition impedes PFOAs' anion exchange interactions and reduces the removal efficiency of DR4. Finally, a noticeable decrease in adsorption efficiency was observed at pH 3. Considering the pK_a of PFOA, at pH 3, approximately 76% of it remains in its non-ionized form. As a result, its electrostatic attraction to the resin is reduced due to the lower negative charge. Additionally, this decrease in adsorption may also be attributed to the presence of chloride ions from the HCl used to acidify the solution, which could compete with PFOA for adsorption sites.[21]

3.5 Effect of inorganic salts and natural organic matter on PFOA adsorption

In addition to the pH study, the selectivity of DR4 for the removal of PFOA was examined in the presence of various inorganic salts and natural organic matter. These competitive adsorption studies included common anions found in drinking and groundwater, such as chloride, nitrate, sulfate, and chromate, using NaCl, $NaNO_3$, Na_2SO_4, and K_2CrO_4 as their respective sources. Additionally, the impact of natural organic matter (NOM) was represented by humic acid and tannic acid was investigated (Fig. 6b). In each experiment, PFOA, and each inorganic salt or NOM were dissolved in Milli-Q water. For each sample, 10 mg of DR4 was used as the sorbent. The concentration of PFOA was 0.2 mg L^{-1} and for each salt or NOM the concentration was 5 mg L^{-1}. The total volume for each sample was 20 mL. A control experiment was conducted by adding the same amounts of PFOA and DR4 into Milli-Q water without any additional salts and NOM. Minimal interference from both inorganic and organic pollutants on the PFOA removal efficiency using DR4 was observed (Fig. 6b).

To expand the scope of this study, an experiment was designed by introducing PFOA, DR4, and a mixture of NaCl, $NaNO_3$, Na_2SO_4, K_2CrO_4, humic acid, and tannic acid into Milli-Q water. The concentration of each salt and NOM was maintained at 5 mg L^{-1}, while the concentration of PFOA was 0.2 mg L^{-} and the amount of DR4 used was 10 mg. The total concentration of inorganic salts and NOM in this experiment was 30 mg L^{-1}, which is 150 times higher than that of PFOA. Compared to the control experiment, no salts or NOM, a reduction of approximately 20% in removal efficiency was

observed, attributed to the increased ionic strength of the aqueous solution, which may decrease the interaction between PFOA and the surface of the resin.[49]

Most studies on adsorbents for PFAS removal from water are done using deionized (DI) or Milli-Q water, often neglecting the impact of dissolved components in tap water. Therefore, PFOA was added to locally sourced tap water from Ithaca, NY and DR4 was used to remove it. The concentration of PFOA was 0.2 mg L^{-1} and the DR4 amount used was 10 mg. A decrease of around 26% in the efficiency of DR4 in removing PFOA from tap water was observed, this is likely due to the presence of various components in tap water (total hardness 122 mg L^{-1}, total alkanility 104 mg L^{-1}, chloride 52 mg L^{-1}, sulfate 12 μg L^{-1}, and Nitrate 0.26 mg L^{-1}) that may interfere with the PFAS removal process.[50]

3.6 PFAS removal from aqueous solutions

While PFOA is the most toxic and prevalent PFAS, other PFASs have been found in wastewater and drinking water supplies, therefore we evaluated the ability of DR4 to remove other PFASs at low concentrations. The PFASs used for this experiment were perfluorobutanoic acid (PFBA), perfluorohexanoic acid (PFHA), perfluoro-2-methyl-3-oxahexanoic acid (GenX), perfluorooctanoic acid (PFOA), perfluorooctane sulfonic acid (PFOS), and perfluorodecanoic acid (PFDA) (Fig. 6c). The experiments were conducted separately in Milli-Q water (single solute system) with a 1 h exposure period. In each experiment, 10 mg of DR4 was used as the sorbent, with an initial concentration of 20 μg L^{-1} for each PFAS and a total volume of 100 mL. PFOA, PFOS, and PFDA, characterized by their longer carbon chains, demonstrated significant removal efficiency when treated with DR4. Notably, PFOS exhibited the highest adsorption rate, achieving above 99% removal efficiency after exposure to the resin with only 8 ng L^{-1} remaining in the solution. The performance of DR4 toward PFOS is likely due to PFOS's high hydrophobicity, and its higher acidity as compared to other PFASs,[20] which facilitates better ionization and subsequently enhances the affinity of PFOS for DR4. The removal efficiencies for GenX, PFHA, and PFBA ranged between 86% and 93%, proving that in addition to removing long chain PFASs, DR4 is also effective for the removal of PFASs with shorter carbon chains. PFBA is identified as a leachable, short-chain anionic PFAS, which is difficult to remove due to its shorter carbon chain and higher water solubility. Previous studies with the same initial concentration of PFBA (20 μg L^{-1}) in Milli-Q water have demonstrated PFBA removal efficiencies ranging from 23% to 35%, underscoring the challenge of achieving high removal rates for this compound.[30,51] However, this difficulty is notably overcome with DR4, which achieves a removal efficiency of more than 93% for PFBA.

To evaluate the impact of co-existing PFASs on adsorption efficiency, a competitive adsorption study was done using a mixture of PFBA, PFHA, GenX, PFOA, PFOS, and PFDA in a multi-solute system (Fig. 6d). The parameters, including the amount of adsorbent, the concentration of each PFAS, the total volume, and the exposure time, were kept consistent with the single solute experiments. Although the total concentration of PFASs in multi-solute solution was 6 times (120 μg L^{-1}) more than that of single solute experiments, there was no change in removal efficiency for PFBA, PFOA, PFOS, and PFDA. Interestingly, for PFHA and especially GenX, the results of the multi-solute experiment showed an improvement in adsorption efficiency compared to the single-solute experiments. The first layer of PFAS adsorption occurs *via* electrostatic interactions, while the second layer involves hydrophobic interactions between the hydrophobic fluorinated tails of PFAS molecules. After the initial interactions, the surface of DR4 loses some of its electrostatic character as it surrounded by PFAS molecules and becomes more hydrophobic[38] due to the hydrophobic fluorocarbon tails that protrude from the PFAS adsorbed onto the resin.[35] Thus longer-chain PFAS continue to be attracted to DR4, leading to higher adsorption efficiency compared to short-chain PFAS.[52,53] Therefore, hydrophobic interactions between GenX and the resin are enhanced by the increased hydrophobicity of the resins in a solution with a variety of PFAS molecules. These results strongly support the synergistic effect of co-existing PFAS on the adsorption efficiency of DR4.

The average concentration of PFAS in contaminated groundwater is close to 1 μg L^{-1}, therefore we evaluated DR4 for PFAS removal at these concentrations.[12] A mixture of PFBA, PFHA, GenX, PFOA, PFOS, and PFDA was added to Milli-Q water at an initial concentration of each PFAS of 200 ng L^{-1}, the amount of DR4 used was 50 mg, the total volume was 20 mL, and the exposure time to the resin was 1 hour. In this solution, the total concentration of PFAS was 1.2 μg L^{-1}, which is close to the average concentration of PFAS in contaminated groundwater.[54] All PFAS, except GenX which had a final concentration of 3.2 ng L^{-1}, were not detected in the solution after exposure to the resin. These samples were analyzed by Pace company using LC/MS-MS and the detection limits for each PFAS were: PFBA 8.4 ng L^{-1}; PFHA 1.4 ng L^{-1}; GenX 2.4 ng L^{-1}; PFOA 4.1 ng L^{-1}; PFOS 1.6 ng L^{-1}; and PFDA 2.2 ng L^{-1}.

In a similar study to PFOA in tap water, DR4's efficacy for a competitive adsorption was studied by adding the PFAS to Ithaca, NY tap water. A sample of tap water direct from the tap was analyzed to ensure that none were detected before the study.

A mixture of PFBA, PFHA, GenX, PFOA, PFOS, and PFDA was added to tap water at an initial concentration of each PFAS of 200 ng L^{-1}, the amount of DR4 used was 50 mg, the total volume was 20 mL, and the exposure time to the resin was 1 hour. Despite the dissolved components in tap water impacting the adsorbent, the results indicated that DR4 performed well toward the removal of PFASs from tap water (Fig. 6e). For instance, in addition to PFDA, PFOS was not detected in the tap water after exposure to DR4. The final concentration of PFOA was measured at 75 ng L^{-1}, indicating a significant reduction. Additionally, the concentrations of PFBA, PFHA, and GenX, decreased to 59, 45, and 61 ng L^{-1}, respectively. These findings confirm the practical application of DR4 in removing PFASs from contaminated drinking water.

3.7 Reusability

The reusability of resins for water purification is important for real-use applications. To assess this, DR4 was evaluated after several consecutive adsorption/desorption cycles. Following previously recognized procedures for regenerating anion exchange resins,[21,23] desorption was conducted using a mixture of methanol and NaCl solution. The quantities of adsorbed PFOA were measured in each cycle. Results from five cycles indicated that DR4 maintained high efficiency (>99%) for PFOA adsorption, demonstrating excellent structural integrity and resilience through successive adsorption–desorption processes (Fig. 6f).

4. Conclusion

In summary, the synthesis and characterization of a new cross-linked anion exchange resin (DR4) by inverse suspension polymerization of APTMAC, a commercially available cationic monomer, in corn oil, cross-linked using BisAAm was reported. To increase the porosity of the resin, PVOH was used as a porogen, and AOT was used as an anionic surfactant to enhance the functionality of ammonium groups on the surface of the resin. Resin DR4 exhibited fast and efficient adsorption capabilities towards various PFAS from contaminated water. The high adsorption capacity of 3300 mg g^{-1} for PFOA, coupled with rapid adsorption kinetics and high selectivity, is attributed to the cationic surface of DR4, which facilitates electrostatic interactions and anion-exchange ability with PFAS. Furthermore, the high swelling of DR4 enhances the mass transfer of PFASs towards the resin in aqueous solutions, thereby achieving fast adsorption of PFASs from water. Additionally, resin DR4 demonstrated excellent regeneration and reusability, maintaining its performance across multiple cycles of reuse. This underscores its practical application for the removal of PFASs from contaminated water sources.

Author contributions

L.K.: conceptualization, formal analysis, data curation, methodology investigation, writing – original draft, writing – review & editing. A.Z.: formal analysis, methodology investigation, data curation, writing – original draft, writing – review and editing. A.A.: project administration, conceptualization, resources, funding acquisition, supervision, writing – review and editing.

Data availability

Raw data used to create the visual elements can be found at: **https://zenodo.org/records/13984331**.

Conflicts of interest

There are no conflicts of interest to declare.

Acknowledgements

We thank the Cornell Center for Materials Research (funded by the National Science Foundation under grant DMR-1719875) and the NMR facility at Cornell University (supported by the NSF through MRI grant number CHE-1531632).

References

1 C. T. Vu and T. Wu, *Crit. Rev. Environ. Sci. Technol.*, 2022, **52**, 90–129.
2 F. Pérez, M. Nadal, A. Navarro-Ortega, F. Fàbrega, J. L. Domingo, D. Barceló and M. Farré, *Environ. Int.*, 2013, **59**, 354–362.
3 N. M. Crawford, S. E. Fenton, M. Strynar, E. P. Hines, D. A. Pritchard and A. Z. Steiner, *Reprod. Toxicol.*, 2017, **69**, 53–59.
4 J. Stone, P. Sutrave, E. Gascoigne, M. B. Givens, R. C. Fry and T. A. Manuck, *Am. J. Obstet. Gynecol. MFM*, 2021, **3**, 100308.
5 L. Cao, Y. Guo, Y. Chen, J. Hong, J. Wu and J. Hangbiao, *Chemosphere*, 2022, **296**, 134083.
6 M.-A. Verner, A. E. Loccisano, N.-H. Morken, M. Yoon, H. Wu, R. McDougall, M. Maisonet, M. Marcus, R. Kishi and C. Miyashita, *Environ. Health Perspect.*, 2015, **123**, 1317–1324.
7 Q. Wu, X. Coumoul, P. Grandjean, R. Barouki and K. Audouze, *Environ. Int.*, 2021, **157**, 106232.
8 B. Granum, L. S. Haug, E. Namork, S. B. Stølevik, C. Thomsen, I. S. Aaberge, H. van Loveren, M. Løvik and U. C. Nygaard, *J. Immunotoxicol.*, 2013, **10**, 373–379.
9 J. C. DeWitt, *Toxicological effects of perfluoroalkyl and polyfluoroalkyl substances*, Springer, 2015.
10 J. L. Domingo and M. Nadal, *J. Agric. Food Chem.*, 2017, **65**, 533–543.
11 P. S. Pauletto and T. J. Bandosz, *J. Hazard. Mater.*, 2022, **425**, 127810.
12 J. Huang, Y. Shi, J. Xu, J. Zheng, F. Zhu, X. Liu and G. Ouyang, *Adv. Funct. Mater.*, 2022, **32**, 2203171.
13 C. Liu, J. Chu, N. L. Cápiro, J. D. Fortner and K. D. Pennell, *J. Hazard. Mater.*, 2022, **422**, 126960.
14 X. Liu, C. Zhu, J. Yin, J. Li, Z. Zhang, J. Li, F. Shui, Z. You, Z. Shi and B. Li, *Nat. Commun.*, 2022, **13**, 2132.
15 D. Q. Zhang, W. L. Zhang and Y. N. Liang, *Sci. Total Environ.*, 2019, **694**, 133606.
16 Y. Liu, T. Li, J. Bao, X. Hu, X. Zhao, L. Shao, C. Li and M. Lu, *Appl. Sci.*, 2022, **12**, 1941.
17 Z. Du, S. Deng, Y. Bei, Q. Huang, B. Wang, J. Huang and G. Yu, *J. Hazard. Mater.*, 2014, **274**, 443–454.

18 E. Gagliano, M. Sgroi, P. P. Falciglia, F. G. Vagliasindi and P. Roccaro, *Water Res.*, 2020, **171**, 115381.
19 P. McCleaf, S. Englund, A. Östlund, K. Lindegren, K. Wiberg and L. Ahrens, *Water Res.*, 2017, **120**, 77–87.
20 A. Maimaiti, S. Deng, P. Meng, W. Wang, B. Wang, J. Huang, Y. Wang and G. Yu, *Chem. Eng. J.*, 2018, **348**, 494–502.
21 Y. Gao, S. Deng, Z. Du, K. Liu and G. Yu, *J. Hazard. Mater.*, 2017, **323**, 550–557.
22 W. Wang, X. Mi, Z. Zhou, S. Zhou, C. Li, X. Hu, D. Qi and S. Deng, *J. Colloid Interface Sci.*, 2019, **557**, 655–663.
23 T. Tamanna, P. J. Mahon, R. K. Hockings, H. Alam, M. Raymond, C. Smith, C. Clarke and A. Yu, *Appl. Sci.*, 2023, **13**, 6263.
24 D. Abdullatif, A. Khosropour, A. Khojastegi, I. Mosleh, L. Khazdooz, A. Zarei and A. Abbaspourrad, *ACS Appl. Polym. Mater.*, 2022, **5**, 412–419.
25 A. Yang, C. Ching, M. Easler, D. E. Helbling and W. R. Dichtel, *ACS Mater. Lett.*, 2020, **2**, 1240–1245.
26 C. Ching, Y. Ling, B. Trang, M. Klemes, L. Xiao, A. Yang, G. Barin, W. R. Dichtel and D. E. Helbling, *Water Res.*, 2022, **209**, 117938.
27 W. Ji, L. Xiao, Y. Ling, C. Ching, M. Matsumoto, R. P. Bisbey, D. E. Helbling and W. R. Dichtel, *J. Am. Chem. Soc.*, 2018, **140**, 12677–12681.
28 J. Huang, Y. Shi, G. Huang, S. Huang, J. Zheng, J. Xu, F. Zhu and G. Ouyang, *Angew. Chem., Int. Ed.*, 2022, **61**, e202206749.
29 A. N. Zeppuhar, D. S. Rollins, D. L. Huber, E. A. Bazan-Bergamino, F. Chen, H. A. Evans and M. K. Taylor, *ACS Appl. Mater. Interfaces*, 2023, **15**, 52622–52630.
30 A. Zarei, A. Khosropour, L. Khazdooz, S. Amirjalayer, A. Khojastegi, A. Zadehnazari, Y. Zhao and A. Abbaspourrad, *ACS Appl. Mater. Interfaces*, 2024, **16**, 9483–9494.
31 W. Wang, A. Maimaiti, H. Shi, R. Wu, R. Wang, Z. Li, D. Qi, G. Yu and S. Deng, *Chem. Eng. J.*, 2019, **364**, 132–138.
32 I. M. Manning, N. G. P. Chew, H. P. Macdonald, K. E. Miller, M. J. Strynar, O. Coronell and F. A. Leibfarth, *Angew. Chem.*, 2022, **134**, e202208150.
33 X. Tan, J. Zhong, C. Fu, H. Dang, Y. Han, P. Král, J. Guo, Z. Yuan, H. Peng and C. Zhang, *Macromolecules*, 2021, **54**, 3447–3457.
34 X. Tan, M. Sawczyk, Y. Chang, Y. Wang, A. Usman, C. Fu, P. Král, H. Peng, C. Zhang and A. K. Whittaker, *Macromolecules*, 2022, **55**, 1077–1087.
35 A. Román Santiago, S. Yin, J. Elbert, J. Lee, D. Shukla and X. Su, *J. Am. Chem. Soc.*, 2023, **145**, 9508–9519.
36 A. Choudhary and D. Bedrov, *ACS Macro Lett.*, 2022, **11**, 1123–1128.
37 S. Anjum, M. Arik, A. Patel, N. Abasali, L. Wu and A. Sarkar, *ACS Appl. Polym. Mater.*, 2025, 1187–1193.
38 A. Zadehnazari, A. Khosropour, A. Zarei, L. Khazdooz, S. Amirjalayer, F. Auras and A. Abbaspourrad, *Small*, 2024, 2405176.
39 L. Khazdooz, A. Zarei, G. Meletharayil, R. Kapoor and A. Abbaspourrad, *ACS Omega*, 2023, **8**, 30966–30975.
40 M. Enayati, M. Karimi Abdolmaleki and A. Abbaspourrad, *ACS Biomater. Sci. Eng.*, 2020, **6**, 2822–2831.
41 R. M. Silverstein, F. X. Webster, D. Kiemle and D. L. Bryce, *Spectrometric Identification of Organic Compounds*, Wiley, 8th Edition, 2014.
42 D. Valade, F. Boschet, S. Roualdès and B. Ameduri, *J. Polym. Sci., Part A: Polym. Chem.*, 2009, **47**, 2043–2058.
43 Z. Shi, K. G. Neoh and E. T. Kang, *Biomaterials*, 2005, **26**, 501–508.
44 R. F. Pereira, R. Brito-Pereira, R. Goncalves, M. P. Silva, C. M. Costa, M. M. Silva, V. de Zea Bermudez and S. Lanceros-Méndez, *ACS Appl. Mater. Interfaces*, 2018, **10**, 5385–5394.
45 S. Yin and D. Villagrán, *Sci. Total Environ.*, 2022, **831**, 154939.
46 B. G. Moneta, M. L. Feo, M. Torre, P. Tratzi, S. E. Aita, C. M. Montone, E. Taglioni, S. Mosca, C. Balducci and M. Cerasa, *Sci. Total Environ.*, 2023, **894**, 165089.
47 G. R. Johnson, M. L. Brusseau, K. C. Carroll and G. R. Tick.
48 Z. Zhang, D. Sarkar, R. Datta and Y. Deng, *J. Hazard. Mater. Lett.*, 2021, **2**, 100034.
49 W. Wang, Z. Zhou, H. Shao, S. Zhou, G. Yu and S. Deng, *Chem. Eng. J.*, 2021, **412**, 127509.
50 **https://www.cityofithaca.org/DocumentCenter/View/15429**.
51 N. Zorigt, A. Zarei, F. Auras, L. Khazdooz, A. Khosropour and A. Abbaspourrad, *Small*, 2024, 2406805.
52 X. Lei, Q. Lian, X. Zhang, T. K. Karsili, W. Holmes, Y. Chen, M. E. Zappi and D. D. Gang, *Environ. Pollut.*, 2023, **321**, 121138.
53 F. Dixit, R. Dutta, B. Barbeau, P. Berube and M. Mohseni, *Chemosphere*, 2021, **272**, 129777.
54 D. Mussabek, A. Söderman, T. Imura, K. M. Persson, K. Nakagawa, L. Ahrens and R. Berndtsson, *Water*, 2022, **15**, 137.